A Development Of Electrode Probes For Imaging Precancerous Lesions With Electrical Impedance Tomography Technique: A Phantom Study

Napatsawan Ngamdi[1], Jaruwan Sriwilai[2], Therdkiat Trongwongsa[2], and Taweechai Ouypornkochagorn[1*]

[1] *Department of Biomedical Engineering, Faculty of Engineering, Srinakharinwirot University, Thailand*
[2] *Department of Pathology, Faculty of Medicine, Srinakharinwirot University, Thailand*
[*] *Corresponding author. E-mail: taweechai@g.swu.ac.th*

Received: January 23, 2023; Accepted: April 15, 2023

Cervical abnormality screening can reduce the risk of getting cancer. Screening methods mostly depend on laboratory investigation which requires equipment, time, and pathologist experience. Electrical bioimpedance has been reported that can be used to identify the presence of cervical intraepithelial neoplasia (CIN) since the conductivity of CIN could be 4-5 times higher than that of normal tissue. In this study, an electrode probe having 8 round electrodes is developed with 1.5 mm-electrode distance. Tissue conductivity can be directly estimated with the probe based on the four-point measurement method, and the image of conductivity distribution can be reconstructed at the same time. The simulation result showed that when tissue thickness was thicker than 4 mm, the commonly-used formula for estimating conductivity is applicable regardless of the electrode shape, but a correction factor was needed with a value up to 1.2 when the thickness was down to 1 mm. The localization performance of the reconstruction images was investigated in a phantom experiment – on a piece of sausage with a burning spot on the surface. Five current excitations were performed from 2 kHz to 125 kHz. The burning surface could be located with a localization error of 0.23 mm with a frequency higher than 2 kHz. However, artifacts were still observable in the images at the boundary region of the electrode array. Thus, increasing the number of electrodes and increasing the probe tip area or decreasing the electrode diameter are still recommended.

Keywords: Electrode probe; Cervical precancerous tissues; Reconstruction; Tissue conductivity

http://dx.doi.org/10.6180/jase.202401_27(1).0006

1. Introduction

Cervical cancer is one leading cause of death in women around the world, and about 90% of cases in 2020 occurred in low– and middle-income countries due to limited access to treatment and public health factors [1]. Regular precancerous cervical screening can reduce the risk of death through early treatment before abnormal tissues progress to cervical cancer. Precancerous cells are classified according to the stage of abnormality development in epithelial which is called Cervical Intraepithelial Neoplasia (CIN), grading into 3 stages i.e. CIN1-3 where CIN3 is the most severe case. Several screening methods have been commonly used to screen and identify the stage of CIN e.g. Pap (Papanicolaou) smear test, liquid-based cytology, pelvic examination, and colposcopy [2, 3]. The Pap smear test is the most popular method in pathological laboratories which uses a spatula to obtain tissue samples from the cervix. The samples are smeared on a slide and the slide will be immersed in 95% ethanol next, and finally, the samples on the slide will be investigated by a microscope. This method is cheap and simple but it has a low sensitivity of about 47.4-51% [3]. Liquid-based cytology (LBC) is an improve-

ment of the Pap smear method proceeded by collecting the tissue samples with a spatula and then putting them into a methanol-based solution. The samples in the solution are prepared to avoid contamination and make cell suspension with an automated machine to produce a thin layer of cells on a slide for microscope investigation. The method can improve the accuracy by 56.6-89.5% [3] however the cost is higher than that of the Pap smear method. The pelvic examination is based on a physical investigation by inserting two gloved fingers inside the vagina while pressing down on the abdomen. In the case of colposcopy, the examination proceeds on the image of the cervix obtained from a colposcope. Apart from these screening methods, Loop Electrosurgical Excision Procedure (LEEP) is another method to verify the presence of CIN or cancer. LEEP is required to biopsy tissue in a woman's lower genital tract with an electric wire loop. Therefore, LEEP is only needed when the screening result shows suspicious or when the treatment plan is undergoing or is determining. The specimen will be investigated by pathologists through the process of clinical diagnosis by cutting it into thin pieces and being entered into the process of making a slide for microscope investigation. The LEEP method unavoidably causes pain and requires about 6 weeks to recover. Overall, all commonly used methods require exhaustive processing time, are relevant with many diagnostics and laboratory equipment, and require experience to obtain the result.

Electrical impedance measurement is another potential method that can screen normal cervical tissues from abnormal tissues [4]. Cell abnormal development on epithelium causes cell enlargement with variation in size and shape resulting in less cell density and change in the electrical property of the cell. The electrical conductivity, at the measurement frequency of 4.8k-614kHz, of the normal cervical tissue was reported at 0.05 S/m but it was 0.19, and 0.26 S/m in the case of CIN1 and CIN2/3, respectively [5, 6] - the abnormality caused higher conductivity by 5 times. This conductivity itself also depends on the frequency used - the conductivity is higher when the measurement frequency increases. For example, when the frequency was changed from 1 kHz to 1 MHz, the conductivity increased by 16 times for the normal tissues and by 4 times for the CIN3 tissue [5]. To measure the conductivity, the measuring apparatus could be in a form of an electrode plate [4, 7] or a probe [5, 6, 8, 9] where a planar electrode array is installed. The electrode plate could be in a form of a well on a planar electrode plate [4] that suits for measuring smear samples, or in a form of a single electrode array plate that suits for measuring the whole piece of LEEP specimen [7]. [5, 6] proposed a 4-electrode probe with 5.5 mm in diameter and 1.65 mm radius of electrode layout. Due to its small diameter, the probe was capable to be used in vivo to determine the presence of CIN by measuring the bioimpedance at 8 locations near the endocervical canal and the squamous epithelial surface. [10] proposed a 16-electrode circular layout of 5 mm in radius while [8] proposed a 9-electrode layout of $\sim$2.83 mm in radius, which all of them have a larger probe tip than [5, 6]. [9] proposed a 7-electrode circular layout of 1.5 mm in radius. which is smaller than [5, 6]. Both [8] and [9] are based on simulation though. They were designed to work with specimens, but they have a high potential to be used in vivo. It is worth noting that, regarding the electrode arrangement, none of them was designed for direct measuring the conductivity with the 4-point measurement technique [11, 12]. To support the 4-point measurement technique, at least 4 electrodes have to be arranged in a straight line with an equal distance of separation. To obtain the precise conductivity value with a probe, further improvement of the reported electrode layouts is necessary.

The 4-point measurement method has the advantage to reduce the effect of contact impedance which is most commonly used [11]. The measurement could be conducted on a tank (with 4 electrode plates inside) or on the surface of tissues. Tissue thickness and electrode separation distance are directly involved in the conductivity estimation. The electrodes are also expected to have a pointed needle tip. However, for physiological measurement, it is difficult to use pointed needle electrodes. [5–10] proposed to use round electrodes where the size was only 0.9-1 mm in diameter, and the distance between electrodes was much smaller than the electrode diameter [5, 6, 10] or about the diameter [7, 9]. Since the shape of these electrodes was round, not pointed, this could introduce a certain value of measurement error because of the significantly large electrode diameter compared to the electrode distance. Furthermore, it could be more complicated with different tissue thicknesses or inhomogeneity.

Imaging conductivity distribution of tissue with the Electrical Impedance Tomography (EIT) technique is an advanced method to use bioimpedance measured from several regions and a variety of measurement patterns. A number of bioimpedance data in conjunction with a mathematic model of tissue are used to reconstruct the image that can be used to address the location of the abnormality. EIT has been used in many medical applications for example lung function monitoring [13] or hemorrhagic stroke monitoring [14]. EIT has the potential to image the biological inhomogeneity of cervixes due to CIN or cancer by a probe. [8, 9] simulated situations where CIN1 or CIN2/3 present

in a circular shape with 1-2 mm in diameter. The larger probe size and more number of electrodes were studied presenting in [8], and the successful localization was found with a localization error of only 0.92 mm. [9] attempted to reduce the probe size (by 56%), which is easier for using to measure in vivo, by decreasing the number of electrodes from 9 to 7. This decrement resulted in an increment of localization error to 1.7 mm ($\sim$2 times increase compared to [9]).

In this study, an improved version of the 7-electrode probe as mentioned in [9] is developed. An electrode was added for conductivity measurement purposes. Apart from 9 opposite patterns used in [9] that were also used in this study, 9 current adjacent patterns were added for improving the sensitivity of conductivity change. The probe, therefore, consists of 8 round electrodes (excluding the ground electrode) fitting in a 15 mm probe tip where 7 of them were arranged in a similar layout to [9] used for the imaging purpose and 1 of them was added and was used with the other electrodes for measuring the tissue conductivity (with the 4-point measurement method) purpose. The probe was investigated with a phantom experiment on 5 frequencies of current excitation. Image reconstruction was conducted to address the abnormality as well as the localization performance was evaluated. The influence of using non-needle electrodes to estimate conductivity was investigated as well.

2. Experimental setup

2.1. EIT machine

The measurement was conducted on an EIT machine developed by ourselves, named "Clementine EIT" (Figure 1). The machine was capable to measure 32 channels, fully parallel, with a signal-to-noise ratio (SNR) over 90dB. The recording speed was 20 frame-per-second, while fixed 5 frequencies of excitation current at 2k, 10k, 25k, 50k, and 125kHz with amplitude of 50, 200, 400, 400, and 400 μArms, respectively, were injected at a frame period, yielding 100 measurement sets (all frequencies) per second.

2.2. Planar electrode probe and electrode configuration

A planar electrode probe to use with the Clementine EIT was developed in this study to be appropriated for cervix application (Figure 2). The probe was circular with 8 round electrodes plus 1 ground electrode. The diameter of the electrodes was 0.9 mm in diameter. The electrode distance was 1.5 mm equally, resulting in 3 mm of the outer electrode ring diameter. The electrodes were installed in a 15 mm-diameter Teflon rod. The rod was stuck with the handle by framing them with polyethylene terephthalate glycol

Fig. 1. The Clementine EIT.

(PETG) material. The position of the 1^{st} electrode to the 7^{th} electrode was consistent with [9]. The 8^{th} electrode was in line with the 1^{st} , the 7^{th} , and the 4^{th} electrode to measure the tissue conductivity regarding the $4-$ point measurement method.

For the reconstruction purpose, the excitation pattern was the mix of the opposite and the adjacent drive configuration (Figure 3a) resulting in 18 driving patterns in total. Nine patterns are in the opposite manner, which are according to [9], and the other 9 patterns are in the adjacent manner. The voltage measurement was based on the adjacent measurement (Figure 3b). The driving electrodes were not used for voltage measurement. Then this configuration yielded 108 composite measurements at a frame. For the conductivity measurement purpose, an extra measurement was added by driving the current from the 1^{st} to the 8^{th} electrode and by measuring the voltage from the 7^{th} and the 4^{th} electrode (Figure 3c). This measurement is according to the 4-point measurement method.

2.3. Phantom experiment

An axial-cut-chicken sausage with 19 mm in diameter and 5 mm in height was used as the phantom in this study. The sausage was kept in a sealed bag in a refrigerator and left outside with the bag at 25 ^{0}C room temperature for 30 minutes before the experiment onset. The EIT measurement was performed by attaching the electrode to the surface of the sausage, at the center, and recorded for 30 seconds. The probe was held in position with a grip holder attached to rods and a stand. The first 0.5 seconds of the record was ignored, resulting in 590 records per frequency. The whole records were averaged to reduce the influence of noise.

The inhomogeneity of the sausage was created by burning the sausage surface with a soldering iron. The tip size

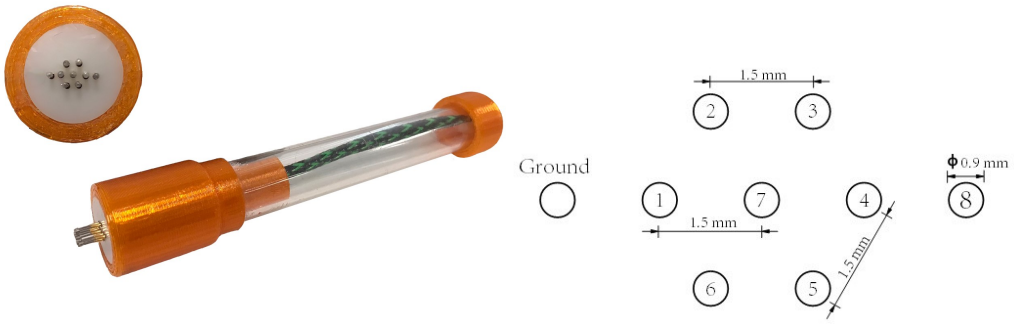

Fig. 2. Electrode probe and its layout.

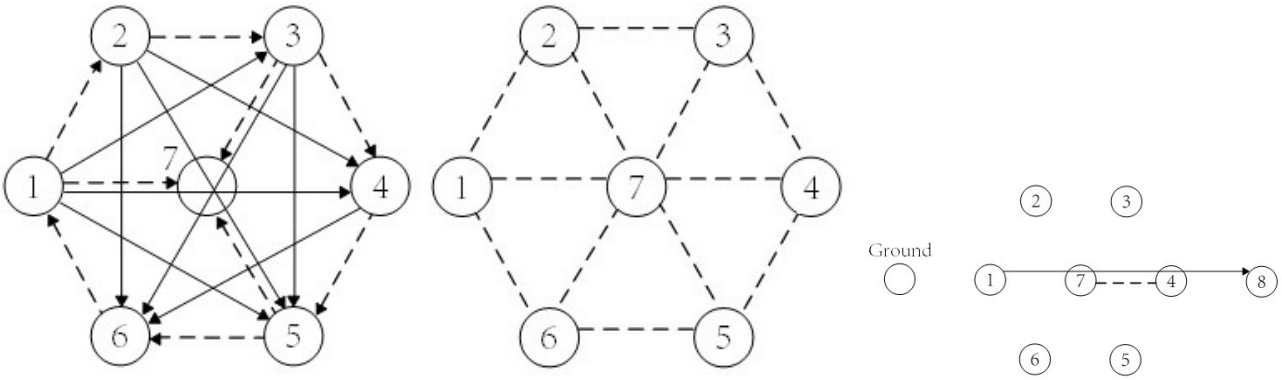

Fig. 3. (a) The current patterns for the reconstruction purpose: the full lines are the opposite patterns and the dash lines are the adjacent patterns, (b) the voltage measurement patterns (the dashed lines) for the reconstruction purpose, and (c) the extra-measurement for the conductivity measurement pattern (the full line is the current pathway and the dashed line is the measurement pair).

was 1.5 mm in diameter. The iron tip was first cleaned with new brass wool and isopropyl alcohol. The soldering iron was set at 380 ^{0}C and then the tip was gently pressed to the surface for 5 seconds. Burning caused the surface to change color but still soft, and the burning shape was circular with ∼2 mm in diameter. The surface was cleaned with a brush damped with 0.9% saline, and the measurement was performed again with the same procedure. The burning surface was expected to be seen in the reconstruction image. To verify the result, the burning surface was situated in different positions of the probe layout. There was only one burning marker on the sausage surface. The probe was moved into 3 positions as shown in Figure 4 and measured on the same piece of the burned sausage. It is worth noting that the center position case (Figure 4b) was not well aligned with the position of the 7th electrode because it is difficult to manipulate due to the small size of the probe.

2.4. Conductivity estimation and image reconstruction

The investigation is divided into 2 parts: tissue conductivity estimation and image reconstruction for the burning surface. For the first part, a method to estimate the tissue conductivity in the condition that the electrode shape was round, not pointed, and the electrode diameter was considerably large compared to the electrode distance was developed. For the second part, the image of inhomogeneity due to burning the surface was reconstructed using measurement data obtained from the developed probe. The conductivity estimation part is involved with the forward computation, while the reconstruction part is involved with both the forward and the inverse computation. Both parts required a mathematical model(s) consistent with the experiment condition.

Twenty-one finite element models were created having a square top surface geometry of 10 mm and 10 mm. The geometry of seven 0.9 mm-diameter electrodes was included

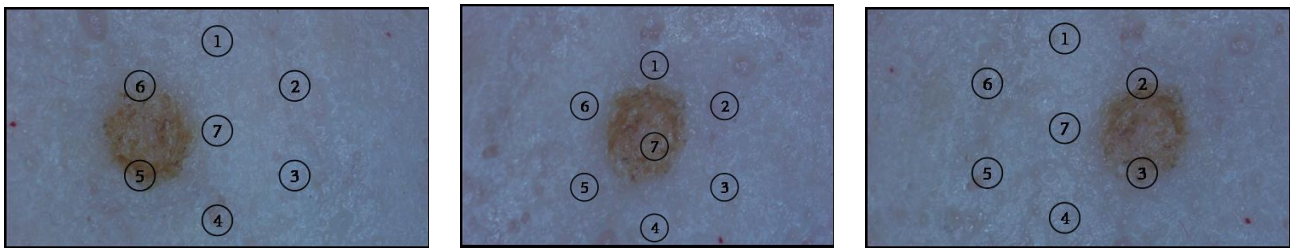

(a) Left **(b)** Center **(c)** Right

Fig. 4. The 3 positions of burned surface regarding the position of the probe in the phantom experiment.

in the first model for reconstructing the burned surface purpose (Figure 5a). The thickness of this model was 5 mm and the number of elements was 30,088. The rest 20 models included the geometry of all eight electrodes for estimating the conductivity. Ten of them used 0.9 mm in electrode diameter, and the others used 0.5 mm instead. The thickness was varied from 1 mm to 10 mm (1 mm in step). The number of elements of these 20 models was between 9,564 to 54,211 (Figure 5b). For all models, the distance of the electrodes to the center electrode (the 7^{th} electrode) was 1.5 mm, and the distance between the 8^{th} electrode to the 4^{th} electrode was also 1.5 mm. Note that, for ease of visual inspection, the geometry of the ground electrode was not included in the models, but the ground electrode was assigned as a pointed electrode at 1.5 mm distance from the 1^{st} electrode (Figure 3c). The model geometries which were in a box shape were different from the true geometry of the sausage which was in a cylinder shape since the probe tip area was significantly small compared to the top surface area of the sausage. This mismatch geometry has a small impact on the accuracy of mathematical computation due to the very small current density flows outside the electrode boundary. The current amplitude for the case of the conductivity estimation was set to 1 mA_{rms}.

In the case of the conductivity estimation, the conductivity of the tissue was set at 0.1, 0.5, 1.0, 1.5, and 2.0 S/m. The simulated tissue was assumed to be put on the non-conductive material. The modified formula for conductivity estimation as in [11] was proposed in (1) where σ is the estimated tissue conductivity, t is the thickness of the tissue, s is the electrode distance (equally separated), V is the measurement voltage, and I is the applied current amplitude. The correction factor $F(t)$, which is a function of t, was added in a similar manner to [12] (since the electrode distance was fixed in this study, the influence of s was not determined here). The correction factor aims to compensate for the change of current density flow manner when the shape of the electrodes is not in a pointed shape. The factor values in regarding different conductivities, thicknesses, and electrode diameters were investigated.

$$\sigma = F(t) \cdot \frac{V}{I} \cdot \pi t \cdot \left(\ln \left(\sinh \left(\frac{t}{s} \right) \cdot \left(\sinh \left(\frac{t}{2s} \right) \right)^{-1} \right) \right)^{-1} \tag{1}$$

In the case of image reconstruction for addressing the burned surface, the conductivity of the sausage was first determined by using (1) with the discover factor value of $F(t)$ at 5 mm thickness and 0.9 mm-diameter of electrodes. The voltage measurement data obtained before and after burning were used, and each of them was averaged over 29.5 seconds of the measurement (the records of the first 0.5 seconds were discarded). The single-step Singular Value Decomposition (SVD) method was used for reconstruction with the regularization parameter (λ) of 1×10^{-4} with (2) and (3), where $\hat{\sigma}$ is the estimated conductivity distribution, $\Delta\hat{\sigma}$ is the different conductivity distribution, U is the model function, I_d is the identity matrix, and J is the Jacobian (sensitivity) matrix. The forward computation was carried out by EIDORS software (http://eidors3d.sourceforge.net/), and the inverse computation was based on the codes developed by the authors.

$$\hat{\sigma} = \arg\min_{\sigma} \left\{ \|V - U(\sigma)\|^2 \right\} \tag{2}$$

$$\Delta\hat{\sigma} = \left(J^T J + \lambda I_d \right)^{-1} J^T (V - U(\sigma)) \tag{3}$$

3. Result

3.1. Conductivity estimation

The values of the correction factor $F(t)$ appeared in (1) regarding different tissue conductivities and thicknesses are shown in Figure 6. When the electrode diameter was 0.9 mm (that is the size used in the developed probe), the factor values decreased from 1.17 at 1 mm-thickness to 0.97 at 10 mm-thickness (20% change) (Figure 6a). The conductivity values had only a slight impact on the factor. When the thickness was ~5 mm, the estimated value was about identical to the formula reported in [11], i.e. the

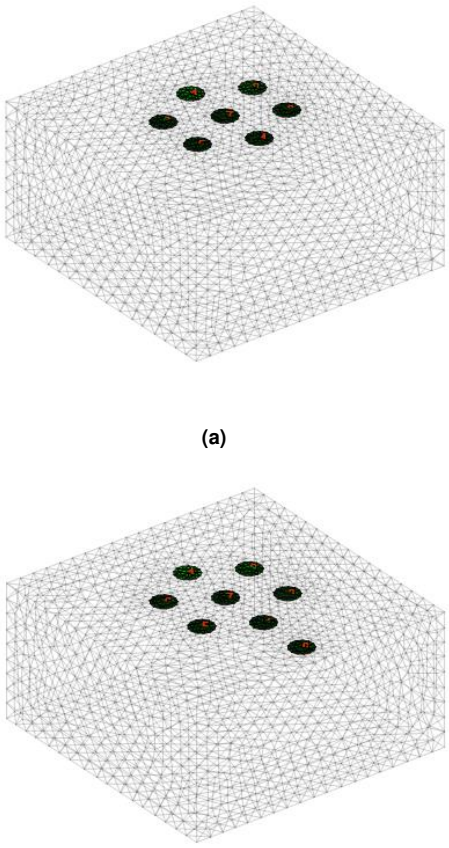

(a)

(b)

Fig. 5. (a) Reconstruction model used for reconstructing and (b) an example of the models used for estimating the conductivity.

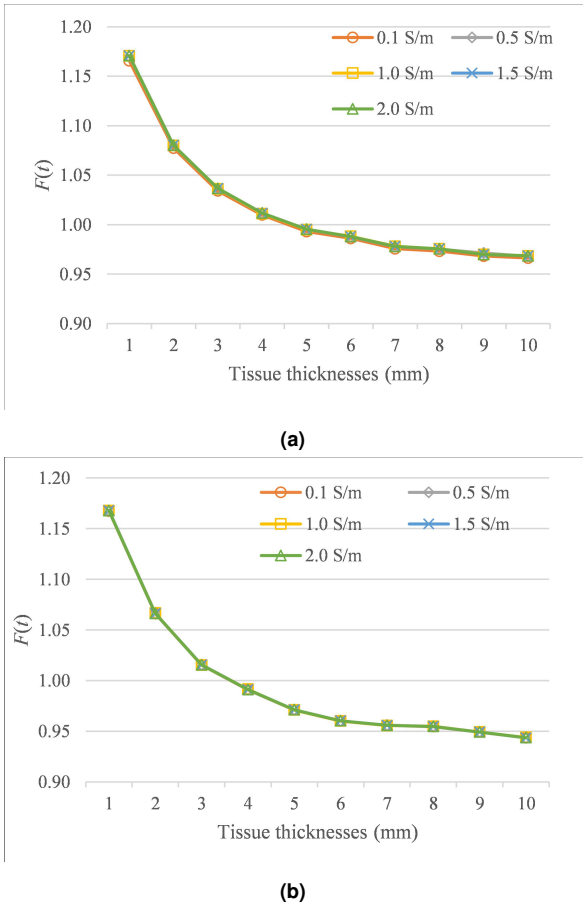

(a)

(b)

Fig. 6. Correction factor over different tissue thicknesses and conductivities of (a) 0.9 mm in electrode diameter (the same size as the electrodes used in the developed probe) and (b) 0.5 mm in electrode diameter.

factor was 0.99. The factor was about unchanged when the thickness was thicker than 6 mm. It is interesting that the decrease in electrode diameter, to be much closer to the point shape, was not significantly different from the 0.9 mm-diameter cases (Figure 6b). The change of the factor was only 0.2 or only 2% smaller.

Since the thickness of the sausage used in this study was 5 mm, the factor is therefore about 1 (i.e. the estimated conductivity value computed by (1) will be about the same when using the formula reported in [11] which is the commonly used one). The measurement data over 29.5 seconds (discarded the first 0.5 seconds) were average and were used to compute the conductivity with the equation (1). The average conductivities are illustrated in Table 1. At the higher frequency, the conductivity was higher. For example, the conductivity at 125 kHz was higher than that of 2 kHz by 14%.

Table 1. The conductivity of a 5 mm-thickness sausage using the correction factor.

Frequency(kHz)	Estimated Sausage Conductivity (S/m)
2	1.077
10	1.125
25	1.159
50	1.190
125	1.223

3.2. Image reconstruction

To reconstruct the image of the burning surface, the model and the estimated conductivity were verified with the measured voltage obtained from the probe first. An example of averaged measurement voltages at 50kHz excitation and the estimated voltages is illustrated in Figure 7. The norms of measurement error were $9(60\%), 18(31\%), 35(31\%), 32(29\%), 33(31\%)$ μV_{rms} for 2k, 10k, 25k, 50k, and 125kHz, respectively.

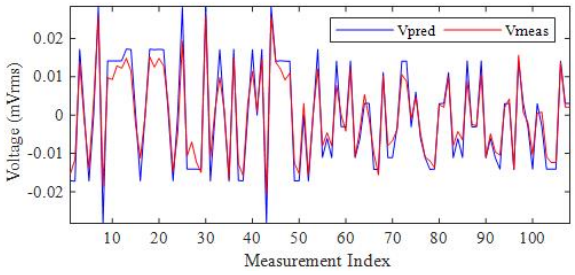

Fig. 7. Comparison between the measurement voltage at 50 kHz excitation (Vmeas) and the estimation voltage computed from the model (Vpred).
[h]

The reconstruction images are shown in Figure 8. Overall, the negative conductivity changes due to burning with the heat on the surface at the left, the center, and the right side can be visualized for almost frequencies. Only the image in the case of burning at the left side and at 2 kHz excitation shows mislocalization. Artifacts as in the positive change can be seen beside the negative change (on the top and the upper region). The amplitude of the change at the 2 kHz case was the smallest i.e. ∼1.5 mS/m. The amplitude at the frequency over 25 kHz was about the same i.e.∼50 mS/m. The localization error of each case is shown in Table 2. Generally, no significant difference among the frequencies over 2 kHz. The average error was 0.17 mm for the frequencies over 2 kHz, but it was 0.82 mm for the 2 kHz cases.

Table 2. The localization error.

Frequency (kHz)	Localization error (mm)		
	Left	Center	Right
2	1.5827	0.5692	0.2935
10	0.1337	0.2285	0.1337
25	0.1337	0.2285	0.1337
50	0.1337	0.2285	0.1337
125	0.1337	0.2285	0.1337

4. Discussions

4.1. Influence of electrode shape on the 4-point measurement method

The 4-point method is a common method to estimate the conductivity of tissue, however, principally it is based on the use of pointed electrodes [11, 12]. In this study, the situation where the electrodes were round and considerately large compared to the electrode distance was investigated. The electrode probe was improved to be able to measure the conductivity while the voltage data were collected for reconstruction. Surprisingly when the thickness of tissue was thicker than ∼4 mm, the round shape (with a diameter of 0.5 mm and 0.9 mm) of electrodes had only a slight difference to what is calculated from the common use formula i.e. [11], regardless of the conductivity values. However, when the thickness was thinner, this could impact up to 20% of the estimated value without factor. The correction values presented in this study then can help in this situation. This observation is in a similar manner to [12] where the correction factor could reduce by 10% when the thickness was reduced to 1 mm. This could indicate that the thin thickness has more influence to the estimation when the round electrode was used.

4.2. Boundary voltage estimation accuracy

The experimental result showed that the estimated voltage data based on a box-shape model and the estimated conductivity were consistent with the measured voltage data. However since the electrode distance was considerately small i.e. 1.5 mm, the voltage magnitude was then reflected as very small. The magnitude norm of the measurement voltage at the 2 kHz cases was only 16 μV_{rms}, while it was 110 μV_{rms} at the 125kHz cases. The system is then easy to be contaminated with noise during measurement and the quantization error of the analog-todigital process has also a large impact on measurement accuracy. In the 2 kHz cases, the norm estimation error was a mere 9 μV_{rms}, but it was 60 % in error. This is because the current amplitudes used in this study were very small i.e. 50, 200, 400, 400, and 400 μArms, at 2k, 10k, 25k, 50k, and 125 kHz, respectively. Therefore, to improve the system, these amplitudes are recommended to be increased to reduce the noise and the quantization error. However, the sensitive region on measured tissues may be a larger resulting complication to reconstruct the change at the surface region. For example, the change in the deeper region may cause artifact at the surface region and then makes it difficult to interpret the image.

4.3. Reconstruction performance and localization accuracy

The reconstruction images based on the developed probe showed satisfactory to localize the burning region with a localization error of less than 0.17 mm at frequencies higher than 2 kHz and than 0.82 at the 2 kHz. The burning region was shown with negative conductivity change which is rational since the burning caused the loss of water content [15]. The localization of the 2 kHz cases was poorer due to the higher noise ratio and quantization error which is rooted in the use of a very small excitation of 50 μArms.

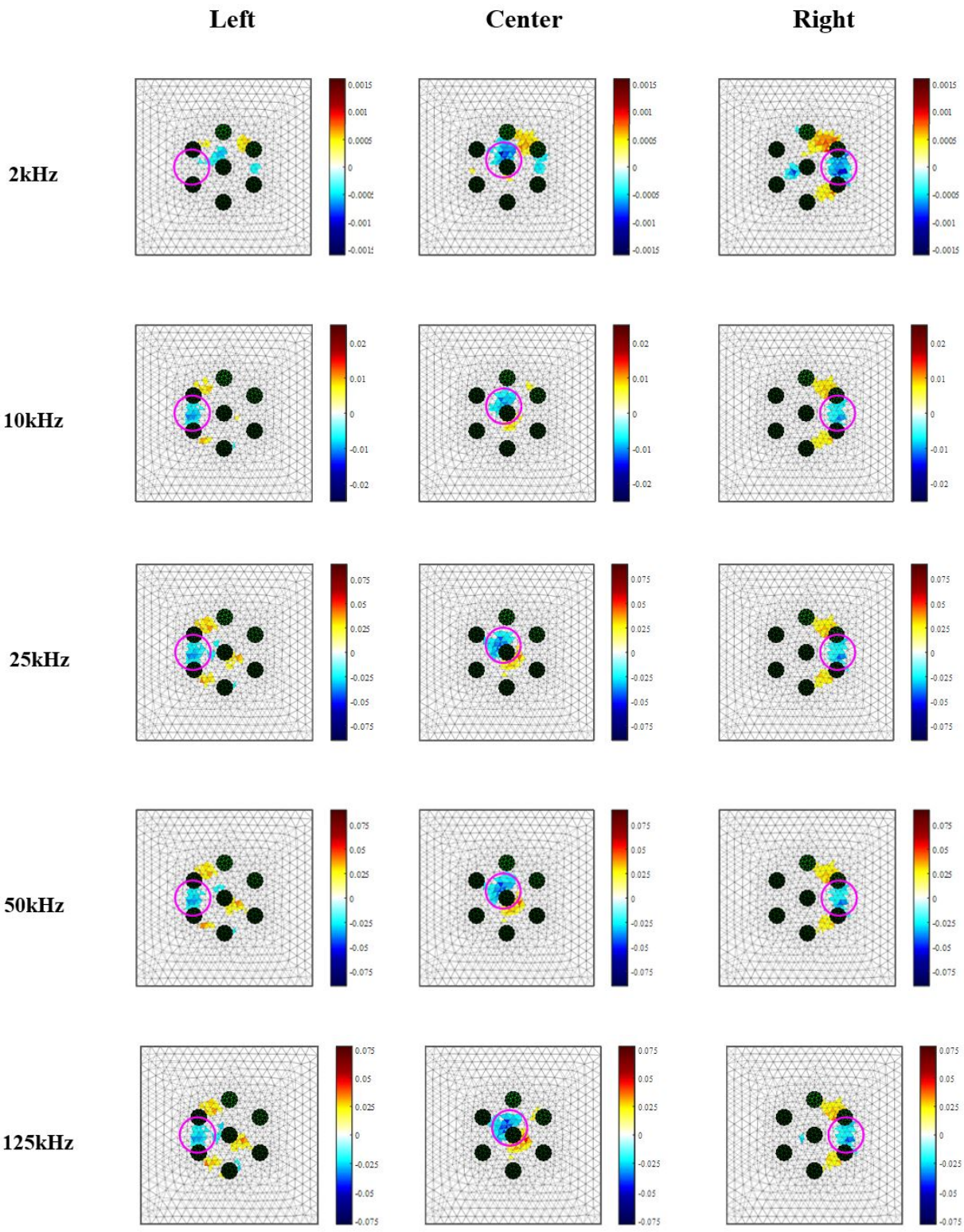

Fig. 8. The reconstruction images of burning on a sausage surface.

Since the highest current amplitude used in this study was 400 μArms which still be considerately small, the artifact is then observable in all images (but it is particularly larger for the 50 μArms case).

Considering the area of the electrode tip i.e. 11.94 mm^2 and the total area of electrode contacts i.e. 4.45 mm^2, the area of the electrode contacts is in a large ratio i.e. 37% of the electrode tip area. Since the conductivity change beneath the electrode contact cannot be reconstructed, this results in a remaining small area to detect the conductivity change. Decreasing the electrode size or increasing the tip size is then advisable to improve the imaging performance. Furthermore, the artifact usually tends to be at the boundary of the image (where the sensitivity is low). To exclude the boundary region from an account, the tip region is then recommended to be increased for avoiding the use of information at the image boundary for interpreting.

The number of electrodes used in the probe is possibly another concern regarding the quality of images. Even though the 7-electrode configuration used in this study yields sufficient image quality, the number of used electrodes limits the number of measurements to only 108 measurements. To obtain more measurement data, using a higher number of electrodes could improve the performance as well. However, this will result in a larger tip which will be harder to be used to measure in vivo.

5. Conclusion

In this study, an electrode probe supporting conductivity measurement with the 4-point measurement method and enabling conductivity distribution reconstruction is purposed. The probe tip was designed to be small for investigating cervixes in vivo. The number of electrodes was 7 plus an extra electrode: 7 of them were used for image reconstruction and the extra one was used with the others for measuring the conductivity – all were round electrodes. The electrode distance was 1.5 mm. Five current excitation frequencies were used. Correction factor towards the common-used formula for conductivity estimation in the situation using round electrodes was studied, and the localization performance of reconstruction images was investigated.

When round electrodes were used to measure the conductivity on the tissue surface, the correction factor had almost no need if the tissue thickness was thicker than 4 mm regardless of the electrode diameters or the tissue conductivity. The factor could be up to 1.2 when the thickness was down to 1 mm. The mathematical model based on the estimated conductivity showed precise voltage estimation. However, the small voltage amplitude due to the small electrode distance and the use of small excitation current amplitude resulted in higher susceptibility to noise and quantization error. According to the phantom experiment result, the measurement data obtained from the probe can still be used to reconstruct the conductivity change on a sausage surface with a localization error of less than 0.17 mm. Artifact, however, appeared on the boundary. Therefore, increasing the excitation current amplitude, increasing the number of electrodes, increasing the electrode tip area, or reducing the electrode diameter are recommended here. These findings would be beneficial for probe improvement in the future. Experimenting on cervical specimens is also necessary to validate the performance of the probe as well.

References

[1] H. Sung, J. Ferlay, R. L. Siegel, M. Laversanne, I. Soerjomataram, A. Jemal, and F. Bray, (2021) *"Global cancer statistics 2020: GLOBOCAN estimates of incidence and mortality worldwide for 36 cancers in 185 countries"* **CA: a cancer journal for clinicians *71***(3): 209–249. DOI: 10.3322/caac.21660.

[2] N. Shanmugapriya and P. Devika, (2017) *"Comparing the effectiveness of liquid based cytology with conventional PAP smear and colposcopy in screening for cervical cancer and it's correlation with histopathological examination: a prospective study"* **International Journal of Reproduction, Contraception, Obstetrics and Gynecology *6***(12): 5336–5341.

[3] M. Karimi-Zarchi, F. Peighmbari, N. Karimi, M. Rohi, and Z. Chiti, (2013) *"A comparison of 3 ways of conventional pap smear, liquid-based cytology and colposcopy vs cervical biopsy for early diagnosis of premalignant lesions or cervical cancer in women with abnormal conventional pap test"* **International journal of biomedical science: IJBS *9***(4): 205.

[4] L. Das, S. Das, and J. Chatterjee, (2015) *"Electrical bioimpedance analysis: A new method in cervical cancer screening"* **Journal of medical engineering *2015***: DOI: 10.1155/2015/636075.

[5] S. Abdul, B. Brown, P. Milnes, and J. Tidy, (2005) *"A clinical study of the use of impedance spectroscopy in the detection of cervical intraepithelial neoplasia (CIN)"* **Gynecologic Oncology *99***(3 Suppl 1): S64–S66. DOI: 10.1016/j.ygyno.2005.07.046.

[6] B. H. Brown, J. A. Tidy, K. Boston, A. D. Blackett, R. H. Smallwood, and F. Sharp, (2000) *"Relation between tissue structure and imposed electrical current flow in cervical neoplasia"* **The Lancet *355***(9207): 892–895. DOI: 10.1016/S0140-6736(99)09095-9.

[7] A. Sillaparaya and T. Ouypornkochagorn. "Planar Electrode Configurations of Electrode Plates for the Localization of Cervical Abnormality based on Electrical Impedance Tomography (EIT)–A Simulation Study". In: *2021 11th International Conference on Biomedical Engineering and Technology*. 2021, 27–33. DOI: 10.1145/3460238.3460243.

[8] S. Ousub, P. Chumjai, A. Sillaparaya, and T. Ouypornkochagorn. "A Simulation Study to Locate Cervical Abnormality based on Electrical Impedance Tomography (EIT), using a Planar Nine-Electrode Probe". In: *2021 11th International Conference on Biomedical Engineering and Technology*. 2021, 1–6. DOI: 10.1145/3460238.3460239.

[9] S. Jankhaboun, W. Janrit, N. Ngamdi, T. Trongwongsa, and T. Ouypornkochagorn. "Planar Electrode Probe Patterns for Cervical Precancerous Screening using Electrical Impedance Tomography". In: *2022 International Electrical Engineering Congress (iEECON)*. IEEE. 2022, 1–4. DOI: 10.1109/iEECON53204.2022.9741605.

[10] T. Zhang, Y. Jeong, D. Park, and T. Oh, (2021) *"Performance Evaluation of Multiple Electrodes Based Electrical Impedance Spectroscopic Probe for Screening of Cervical Intraepithelial Neoplasia"* **Electronics *10***(16): 1933. DOI: 10.3390/electronics10161933.

[11] D. K. Schroder. *Semiconductor material and device characterization*. John Wiley & Sons, 2015.

[12] L. B. Valdes, (1954) *"Resistivity measurements on germanium for transistors"* **Proceedings of the IRE *42***(2): 420–427. DOI: 10.1109/JRPROC.1954.274680.

[13] V. Tomicic and R. Cornejo, (2019) *"Lung monitoring with electrical impedance tomography: technical considerations and clinical applications"* **Journal of thoracic disease *11***(7): 3122. DOI: 10.21037/jtd.2019.06.27.

[14] T. Ouypornkochagorn, N. Terzija, P. Wright, J. L. Davidson, N. Polydorides, and H. McCann, (2022) *"Scalp-mounted electrical impedance tomography of cerebral hemodynamics"* **IEEE sensors journal *22***(5): 4569–4580. DOI: 10.1109/JSEN.2022.3145587.

[15] T. Faes, H. Van Der Meij, J. De Munck, and R. Heethaar, (1999) *"The electric resistivity of human tissues (100 Hz-10 MHz): a meta-analysis of review studies"* **Physiological measurement *20***(4): R1. DOI: 10.1088/0967-3334/20/4/201.